Two Tris(imino)tin(II) and -lead(II) Cage Complexes. Syntheses and Structures of E[μ-N=C(^{t}Bu)Ph]$_3$Li·THF (E = Sn, Pb)

Andrew J. Edwards,[†] Michael A. Paver,[†] Paul R. Raithby,[†] Christopher A. Russell,[†] Alexander Steiner,[‡] Dietmar Stalke,[‡] and Dominic S. Wright*,[†]

University Chemical Laboratory, University of Cambridge, Lensfield Road, Cambridge CB2 1EW, U.K., and Institut für Anorganische Chemie, Universität Göttingen, Tammannstrasse 4, W-37077 Göttingen, Germany

Received October 19, 1993[⊗]

The reactions of Cp_2Pb and Cp_2Sn with LiN=C(^{t}Bu)Ph (1:1; 2 or 3 equiv) in THF produce the isostructural complexes Pb[μ-N=C(^{t}Bu)Ph]$_3$Li·THF (**1**) and Sn[μ-N=C(^{t}Bu)Ph]$_3$Li·THF (**2**), respectively. Complex **2** can also be prepared by the facile ligand-exchange reaction of **1** and Cp_2Sn in THF. The crystal structures of both complexes have been obtained at 153 K. Crystal data: **1**, orthorhombic, space group $P2_12_12$, a = 16.912(2) Å, b = 19.214(2) Å, c = 11.212(3) Å, Z = 4; **2**, monoclinic, space group $P2_1/n$, a = 10.679(2) Å, b = 33.036(7) Å, c = 10.683(2) Å, β = 106.84(3)°, Z = 4. Both complexes have monomeric trigonal bipyramidal EN_3Li cage structures (E = Pb, Sn) in which there are sharp (*ca.* 80°) angles at the bridging imino-N centers and close intermolecular E···Li contacts which are slightly greater than the sum of the covalent radii of the metals [2.85(3) in **1** and 2.776(4) Å in **2**]. Model semiempirical (MNDO) calculations suggest that there is no significant E–Li bonding in either complex and that the observed core geometries mainly reflect the optimal bridging angle of the imino ligands. Monomer molecules of **1** exhibit extreme angular distortions within the PbN_3Li core, resulting from two such molecules pairing up in the lattice. Their phenyl groups intermesh, and long-range (*ca.* 3.26 Å) (*ortho*)C—H···Pb contacts are established. In contrast, molecules of **2** have a largely symmetrical core and do not associate in the manner of those of **1** in the solid state. This unexpected structural difference between **1** and **2** may suggest that the (*ortho*)C—H···Pb contacts observed in **1** are more than simply van der Waals interactions.

Introduction

We recently synthesized and structurally characterized compounds of the group 14 heavy p block metals (Sn, Pb).[1] The [(Ph_3E)Li·PMDETA] complexes {E = Sn, Pb; PMDETA = $[(CH_3)_2NCH_2CH_2]_2NCH_3$} contain the first structually authenticated early main group metal–heavy p block metal bonds.[1] The structure of the Sn–K-bonded complex ((^{t}BuCH$_2$)$_3$Sn)K·3-(toluene) was also recently reported by Lawless and co-workers.[2] Such triorganostannates and plumbates are valuable precursors in organic synthesis.[3] More recently, we were interested in the synthetic utility of heavy p block metal cyclopentadienide complexes as precursors to organometallics and anionic metal ('ate) complexes. Nucleophilic *addition* of CpNa or Cp_2Mg (Cp = C_5H_5) to Cp_2E produces ion-separated and ion-contacted complexes containing unusual Cp_3E^- "paddle wheel" ions.[4] However, the reaction between Cp_2Sn and LiN=C(NMe_2)$_2$ (1:1 equiv) results in nucleophilic *substitution* of one of the cyclopentadienide ligands and leads to the formation of the dimeric mixed-ligand complex {(η^3-Cp)Sn[μ_2-N=C(NMe_2)$_2$]}$_2$.[5] With more potent nucleophiles and Cp_2Sn, we found that substitution proceeds a stage further, leading to triorganostannates. Hence, the reaction of FlLi (Fl = fluoren-9-yl, $C_{13}H_9$) with Cp_2Sn (2:1 or 3:1 equiv) in THF results in disubstitution followed by addition of a third Fl ligand and in the formation of [(η^1-Fl)$_3$Sn]$^-$[Li(THF)$_4$]$^+$.[6] We also recently communicated the synthesis and structure of Pb[μ-N=C(^{t}Bu)Ph]$_3$Li·THF, which was prepared by a similar route from Cp_2Pb.[7] The complex has a trigonal bipyramidal PbN_3Li cage structure in the solid state in which a short Pb···Li contact is found and in which long-range intermolecular (*ortho*)C—H···Pb interactions are present between molecular pairs in the crystal.

We here report a full account of the synthesis and structure of Pb[μ-N=C(^{t}Bu)Ph]$_3$Li·THF (**1**), the first imino Pb complex and the first structually characterized triorganoplumbate containing Pb–N bonds. The synthesis of the Sn(II) analogue Sn[μ-N=C(^{t}Bu)Ph]$_3$Li·THF (**2**) is reported from a route similar to that producing **1** and from a facile metal-interchange reaction from **1** and Cp_2Sn (1:1 equiv). Although the molecular structures of **1** and **2** are both monomeric trigonal bipyramidal cages, there are no significant intermolecular contacts within the structure of **2**. This difference between **1** and **2** suggests that the (*ortho*)-C—H···Pb contacts observed in **1** may be more than simply van der Waals interactions.

Results and Discussion

Syntheses of 1 and 2. The product complexes and starting materials involved in this work are all air and/or moisture sensitive. The reactions discussed were carried out, in the manner described

[†] University of Cambridge.
[‡] Universität Göttingen.
[⊗] Abstract published in *Advance ACS Abstracts,* April 15, 1994.

(1) (a) Reed, D.; Stalke, D.; Wright, D. S. *Angew. Chem.* **1991**, *103*, 1539; *Angew. Chem., Int. Ed. Engl.* **1991**, *30*, 1459. (b) Armstrong, D. R.; Davidson, M. G.; Moncrieff, D.; Stalke, D.; Wright, D. S. *J. Chem. Soc., Chem. Commun.* **1992**, 1413.
(2) Hitchcock, P. B.; Lappert, M. F.; Lawless, G. A.; Royo, B. *J. Chem. Soc., Chem. Commun.* **1993**, 554.
(3) (a) Fieser, M. *Reagents for Organic Synthesis;* Wiley: New York; Vol. 15 and earlier volumes. (b) Pereyre, M.; Quintard, J.-P.; Rahm, A. *Tin in Organic Synthesis;* Butterworths: London, 1987. (c) Omae, I. *Organotin Chemistry;* Elsevier: Amsterdam, 1989. (d) Yamamoto, Y., Ed. Organotin Compounds in Organic Synthesis. *Tetrahedron* **1989**, *45*, 909. (e) Harrison, P. *Chemistry of Tin;* Chapman and Hall: New York, 1989.
(4) (a) Davidson, M. G.; Stalke, D.; Wright, D. S. *Angew. Chem.* **1992**, *104*, 1265; *Angew. Chem., Int. Ed. Engl.* **1991**, *31*, 1226. (b) Armstrong, D. R.; Davidson, M. G.; Moncrieff, D.; Russell, C. A.; Stalke, D.; Steiner, A.; Wright, D. S. *J. Am. Chem. Soc.,* submitted for publication.
(5) Stalke, D.; Paver, M. A.; Wright, D. S. *Angew. Chem.* **1993**, *105*, 445; *Angew. Chem., Int. Ed. Engl.* **1993**, *32*, 428.
(6) Edwards, A. J.; Paver, M. A.; Raithby, P. R. R.; Russell, C. A.; Steiner, A.; Stalke, D.; Wright, D. S. *J. Chem. Soc., Dalton Trans.* **1993**, 1465.
(7) Edwards, A. J.; Paver, M. A.; Raithby, P. R.; Russell, C. A.; Wright, D. S. *J. Chem. Soc., Chem. Commun.* **1993**, 1349.

0020-1669/94/1333-2370$04.50/0

Scheme 1

$$Cp_2E + xLiN{=}C(^tBu)Ph \xrightarrow[E=Sn,\,Pb;\,x=1\text{-}3]{THF} E[(\mu\text{-}N{=}C(^tBu)Ph]_3Li{\cdot}THF$$

Scheme 2

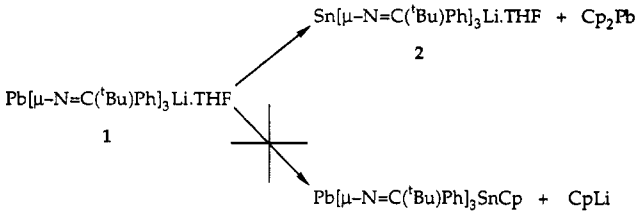

in the Experimental Section, under dry O_2 free N_2 on a vacuum line, and **1** and **2** were isolated and handled using a glovebox.[8] Complexes **1** and **2** can both be prepared cleanly (**1** in 67% and **2** in 25% yield) by the reactions of Cp_2Pb and Cp_2Sn, respectively, with LiN=C(ᵗBu)Ph in THF as solvent (Scheme 1). Surprisingly, a 1:1 or 1:2 ratio of Cp_2E (E = Sn or Pb) to LiN=C(ᵗBu)Ph gives complex **1** or **2**, in which substitution of both Cp ligands followed by addition of a third has occurred. It therefore appears that mono- and disubstitution of Cp_2E by this imino anion is not possible. This situation is in contrast with that of the 1:1 reaction of Cp_2Sn with $LiN{=}CN(Me_2)_2$ in THF, which yields only the monosubstitution product $\{(\eta^3\text{-}Cp)Sn[\mu\text{-}N{=}C(NMe_2)_2]\}_2$.[5] Although **1** and **2** were obtained using the correct 1:3 ratios of reactants, these reactions are far less clean and the products less easily crystallized than those with the reduced ratio of the imino anion.

Remarkably, the reaction of complex **1** with Cp_2Sn, instead of producing the desired mixed Pb/Sn cage complex and CpLi, produces complex **2** (30%) (Scheme 2). Thus facile metal interchange of Pb for Sn has been achieved by ligand transfer of all three N=C(ᵗBu)Ph groups from Pb to Sn, presumably producing Cp_2Pb. The driving force for this reaction is probably the relative strength of the Sn–N bonds in **2** over the weak Pb–N bonds in **1**.

Crystal Structures of 1 and 2. Complexes **1** and **2** were characterized by IR and ^1H and ^{13}C NMR spectroscopy and by elemental analyses (C, H, N) prior to obtaining their crystal structures by low-temperature single-crystal X-ray diffraction analyses. For the latter, crystals of the correct size and quality were grown directly from the reactions described in the Experimental Section and with no other modifications. Details of the X-ray data collections and refinements for both complexes are collected in Table 1. Atomic coordinates (non-H atoms) are given in Tables 2 and 3 for **1** and **2**, respectively, and selected bond lengths and angles for complexes **1** and **2** are shown in Tables 4 and 5, respectively.

$Pb[\mu\text{-}N{=}C(^tBu)Ph]_3Li{\cdot}THF$ (**1**) has a monomeric structure in the solid state (Figure 1). Molecules of **1** contain a trigonal bipyramidal PbN_3Li core in which the bridging imino-N centers link the three-coordinate Pb and four-coordinate (THF-solvated) Li atoms together. The THF molecule exhibits disorder over C(2), C(3), and C(4), and these atoms were finally refined with 50% occupancy over two sites. It is the bridging of the imino-N centers of the Pb and Li atoms which presumably gives rise to the close contact between the two metals rather than any significant Pb–Li bonding in **1** [2.85(3) Å in **1**; cf. 2.858(14) Å in the Pb–Li-bonded monomer $(Ph_3Pb)Li{\cdot}PMDETA$;[1b] sum of covalent radii of Pb and Li 2.81 Å[10]]. Such a trigonal bipyramidal core motif as that seen in the structure of **1** has been observed in several early main group metal (groups 1 and 2) Sn(II) and Pb(II) trialkoxide complexes,[11] e.g., in monomeric $Sn(2,6\text{-}DPP)_3Li$ (DPP = diphenylphenoxide).[11a] However, there are no structurally characterized triorgano derivatives containing Pb–N bonds and **1** is the first imino Pb complex to be structurally characterized.

Table 1. Crystal Data and Structure Solutions of $Pb[\mu\text{-}N{=}C(^tBu)Ph]_3Li{\cdot}THF$ (**1**) and $Sn[\mu\text{-}N{=}C(^tBu)Ph]_3Li{\cdot}THF$ (**2**)

	1	**2**
empirical formula	$C_{37}H_{50}LiN_3OPb$	$C_{37}H_{50}LiN_3OSn$
fw	766.94	678.43
T (K)	153(2)	153(2)
λ (Å)	0.710 73	0.710 73
crystal system	orthorhombic	monoclinic
space group	$P2_12_12$	$P2_1/n$
a (Å)	16.912(2)	10.679(2)
b (Å)	19.214(2)	33.036(7)
c (Å)	11.121(2)	10.683(2)
α (deg)	90	90
β (deg)	90	106.84(3)
γ (deg)	90	90
V (Å^{-3})	3613.7(11)	3607.3(12)
Z	4	4
ρ_{calc} (Mg m^{-3})	1.409	1.249
transm coeff	0.665–0.294	0.781–0.715
R indices $[F > 4\sigma(F)]^a$	wR1 = 0.054, wR2 = 0.1635	wR1 = 0.025, wR2 = 0.067
R indices (all data)^a	wR1 = 0.068, wR2 = 0.2071	wR1 = 0.028, wR2 = 0.070

^{a} $wR1 = \sum||F_o| - |F_c||/\sum|F_o|$ and $wR2 = \{[\sum w(F_o^2 - F_c^2)^2]/\sum wF_o^4\}^{0.5}$; $w = 1/[\sigma^2(F_o^2) + (xP)^2 + yP]$, $P = (F_o^2 + 2F_c^2)/3$.[9]

Within the core of **1**, the Pb–N and Li–N distances fall within the expected ranges [average Pb–N 2.332(17) Å; average Li–N 2.08(3) Å].[12,13] However, there are large angular distortions at N(2)–Pb(1)–N(1) [81.6(5)°; cf. average 74.1° for the other N–Pb–N angles] and at N(1)–Li(1)–N(2) [95(1)°; cf. 85(1)° for the other two N–Li–N angles]. These angular distortions result from the way in which molecules of **1** are associated in the solid state. Two such monomeric units intermesh their phenyl rings at their open [Pb(1)N(1)Li(1)N(2)] faces, and intermolecular aryl (*ortho*)C—H···Pb interactions result (3.26 Å; cf. sum of van der Waals radii of H and Pb 3.2–3.4 Å[10]) (Figure 2).

All three (ᵗBu)(Ph)C=N ligands are orientated with their *tert*-butyl groups facing toward the $Li{\cdot}THF^+$ fragment and their phenyl rings facing and surrounding the Pb center in the monomers of **1**. Two of these phenyl groups [associated with the imino ligands at N(1) and N(2)] have centroid···Pb distances (3.86 and 3.83 Å, respectively) which approach the sum of the van der Waals radii of Pb and the arene (estimated *ca.* 3.7 Å[10]). The closest C···Pb contacts (*ca.* 3.21–3.31 Å) are made with the α and *ortho* carbon atoms of these rings. Such distances are much longer than have been observed in $(\eta^6\text{-}C_6H_6)Pb(AlCl_4)_2{\cdot}C_6H_6$ [(centroid)η^6-C_6H_6···Pb(II) 2.77 Å].[14] It should be noted that no ^{13}C···Pb coupling could be observed in the room temperature ^{13}C NMR spectrum of **1** in THF. The relatively close arene···Pb contacts in **1** are most probably a consequence of steric repulsion between the ᵗBu groups of the imino ligands and the Li-attached THF molecule, which forces the imino ligands to pivot toward Pb. Steric repulsion with the ᵗBu groups is presumably largely

(8) Shriver, D. F.; Drezdon, M. A. *The Manipulation of Air-Sensitive Compounds*, 2nd ed.; Wiley: New York, 1986.
(9) Sheldrick, G. M. SHELXL-93. Universität Göttingen, 1993.
(10) (a) Cotton, F. A.; Wilkinson, G. *Advanced Inorganic Chemistry*, 5th ed.; Wiley: New York, 1988; p 283. (b) Bondi, A. *J. Phys. Chem.* **1964**, *68*, 441. (c) Huheey, J. E. *Inorganic Chemistry*, 3rd ed.; Harper and Row: New York, 1983; p 258.
(11) (a) Smith, G. D.; Fanwick, P. E.; Rothwell, I. P. *Inorg. Chem.* **1989**, *28*, 618. (b) Veith, M.; Kafer, D.; Huch, V. *Angew. Chem.* **1986**, *98*, 367; *Angew. Chem., Int. Ed. Engl.* **1986**, *25*, 375. (c) McGeary, M. J.; Cayton, R. H.; Folting, K.; Huffman, J. C.; Caulton, K. G. *Polyhedron* **1992**, *11*, 1369.
(12) (a) Gregory, K.; Schleyer, P. v. R.; Snaith, R. *Adv. Inorg. Chem.* **1991**, *37*, 47. (b) Mulvey, R. E. *Chem. Soc. Rev.* **1991**, *20*, 167.
(13) Engelhart, L. M.; Furphy, B. M.; Harrowfield, J. M.; Patrick, J. M.; White, A. H. *Inorg. Chem.* **1989**, *28*, 1411.
(14) Gash, A. G.; Rodesiler, P. F.; Amma, E. L. *Inorg. Chem.* **1974**, *13*, 2429.

Table 2. Atomic Coordinates ($\times 10^4$) and Equivalent Isotropic Displacement Parameters ($Å^2 \times 10^3$) for **1**

	x	*y*	*z*	*U*(eq)[a]
Pb(1)	1229(1)	1531(1)	8404	24(1)
Li(1)	1265(19)	1695(13)	5858(23)	22(6)
O(1)	1292(10)	1619(7)	4102(10)	35(3)
C(1)	1309(17)	932(13)	3595(23)	56(6)
C(2)	1079(27)	1066(22)	2287(38)	110(13)
C(3)	938(32)	1786(22)	2135(40)	38(5)
C(3A)	1349(33)	1628(26)	1978(42)	38(5)
C(4)	1373(32)	2079(24)	3131(44)	38(5)
C(4A)	1065(36)	2195(28)	3095(51)	38(5)
N(1)	2159(9)	1291(8)	6910(44)	23(4)
C(11)	2858(11)	1179(9)	7178(17)	23(4)
C(12)	3525(12)	1174(10)	6336(20)	34(6)
C(13)	3198(13)	1197(13)	5047(19)	41(6)
C(14)	4017(12)	1862(12)	6458(22)	42(6)
C(15)	4105(14)	523(13)	6449(26)	52(7)
C(101)	3081(10)	1065(8)	8485(18)	17(4)
C(102)	3164(12)	388(12)	8954(19)	33(5)
C(103)	3313(15)	292(14)	10228(24)	54(6)
C(104)	3406(14)	854(12)	10966(22)	44(6)
C(105)	3293(13)	1523(15)	10505(19)	43(5)
C(106)	3149(11)	1640(11)	9314(17)	29(5)
N(2)	358(8)	1254(7)	6848(14)	21(4)
C(21)	−398(13)	1169(10)	7088(18)	27(5)
C(22)	−1032(12)	1141(13)	6140(20)	39(6)
C(23)	−646(15)	1073(16)	4956(21)	57(8)
C(24)	−1459(14)	1852(13)	6246(22)	49(7)
C(25)	−1593(15)	550(15)	6386(28)	64(8)
C(201)	−664(11)	1145(10)	8426(21)	29(4)
C(202)	−654(13)	1756(11)	9106(20)	37(5)
C(203)	−834(18)	1730(17)	10336(30)	77(9)
C(204)	−1016(21)	1075(18)	10726(34)	84(11)
C(205)	−1010(19)	480(18)	10122(31)	82(9)
C(206)	−857(15)	537(14)	9021(24)	54(7)
N(3)	1226(9)	2496(6)	7140(12)	20(3)
C(31)	1240(12)	3108(9)	7510(14)	24(4)
C(32)	1291(12)	3723(8)	6655(16)	25(4)
C(33)	1266(14)	3477(11)	5338(16)	36(4)
C(34)	615(15)	4251(12)	6813(26)	52(7)
C(35)	2068(15)	4090(12)	6795(24)	49(6)
C(301)	1219(12)	3310(8)	8884(15)	23(4)
C(302)	500(12)	3490(12)	9396(19)	37(5)
C(303)	455(17)	3630(15)	10551(26)	64(8)
C(304)	1098(20)	3624(16)	11222(29)	76(10)
C(305)	1840(13)	3469(14)	10775(20)	44(5)
C(306)	1913(12)	3305(10)	9537(18)	34(5)

[a] *U*(eq) is defined as one-third of the trace of the orthogonalized U_{ij} tensor.

responsible for the bent attachment of the THF ligand to Li [Pb(1)···Li(1)—O(1) *ca.* 170°].

Sn[μ-N=C(^{t}Bu)Ph]$_3$Li·THF (**2**) has a monomeric trigonal bipyramidal cage structure similar to that of **1** in the solid state (Figure 3). However, the SnN_3Li core of **2**, in contrast to the core of **1**, is largely symmetrical in terms of the angles about Sn and Li. It is noticeable also that, whereas the core N–Li–N angles of **1** and **2** are similar (average of 88° in **1** and average of 84.4° in **2**), the N–Sn–N angles of **2** are less acute than the corresponding metal angles found in the core of **1** (average N–Sn–N 79.7° in **2**; cf. average N–Pb–N of 76.7° in **1**). The latter is presumably related to the expected effective increased separation ("inert pair") of the *n*s and *n*p orbitals on going from Sn to Pb and thus to the proportion of p character which each metal employs in bonding to N. The Sn···Li contact in **2** is again only slightly greater than the sum of the covalent radii of Sn and Li [2.776(4) Å in **1**; cf. 2.74 Å[10]]. However, once again the shortness of this contact is a probable consequence of the imino groups, whose natural metal-bridging angle is sharp [average of 81.5° in **2** and average of 80° in **1**; cf. *ca.* 78° in {(η^3-Cp)Sn-[μ-N=C(NMe$_2$)$_2$]}$_2$[5]], holding the Sn and Li together rather than any significant Sn–Li bonding.

In contrast to the core of **1**, where only core angle distortions occur as a consequence of apparent intermonomer association,

Table 3. Atomic Coordinates ($\times 10^4$) and Equivalent Isotropic Displacement Parameters ($Å^2 \times 10^3$) for **2**

	x	*y*	*z*	*U*(eq)[a]
Sn(1)	9936(1)	8894(1)	5857(1)	30(1)
Li(1)	9924(4)	8933(1)	8449(4)	37(1)
N(1)	9152(2)	8483(1)	7012(2)	34(1)
C(1)	8515(2)	8166(1)	6597(2)	34(1)
C(2)	7982(3)	7903(1)	7519(3)	49(1)
C(3)	9099(5)	7823(1)	8749(4)	105(2)
C(4)	6977(5)	8149(2)	7908(5)	126(2)
C(5)	7420(5)	7505(1)	6936(4)	105(2)
C(6)	8213(3)	8024(1)	5201(3)	38(1)
C(7)	7052(3)	8129(1)	4289(3)	56(1)
C(8)	6745(4)	7998(1)	3020(3)	77(1)
C(9)	7601(5)	7758(1)	2646(4)	82(1)
C(10)	8759(5)	7648(1)	3502(4)	77(1)
C(11)	9074(3)	7783(1)	4797(3)	58(1)
N(2)	11496(2)	8927(1)	7715(2)	32(1)
C(12)	12688(3)	8874(1)	7815(2)	32(1)
C(13)	13760(3)	8927(1)	9125(3)	47(1)
C(14)	14079(4)	8507(1)	9714(3)	90(1)
C(15)	15000(3)	9120(2)	8938(3)	76(1)
C(16)	13270(3)	9196(1)	10029(3)	55(1)
C(17)	13113(2)	8732(1)	6668(2)	36(1)
C(18)	13580(3)	8987(1)	5891(3)	50(1)
C(19)	13846(3)	8845(1)	4778(3)	67(1)
C(20)	13645(3)	8443(1)	4446(3)	77(1)
C(21)	13179(4)	8190(1)	5209(4)	79(1)
C(22)	12907(3)	8328(1)	6305(3)	59(1)
N(3)	9092(2)	9322(1)	6932(2)	31(1)
C(23)	8350(2)	9612(1)	6419(2)	31(1)
C(24)	7832(3)	9913(1)	7250(3)	41(1)
C(25)	6366(4)	9980(1)	6639(4)	59(1)
C(26)	8050(5)	9746(2)	8615(4)	61(1)
C(27)	8556(5)	10311(1)	7321(5)	60(1)
C(25′)	7570(29)	10334(6)	6699(16)	100(9)
C(26′)	6673(19)	9711(7)	7465(23)	101(7)
C(27′)	8860(17)	9947(6)	8633(14)	65(4)
C(28)	7876(2)	9668(1)	4958(2)	31(1)
C(29)	7045(2)	9376(1)	4221(3)	43(1)
C(30)	6631(3)	9396(1)	2874(3)	53(1)
C(31)	7048(3)	9708(1)	2246(3)	54(1)
C(32)	7873(3)	9994(1)	2951(3)	49(1)
C(33)	8280(3)	9977(1)	4305(2)	39(1)
O(1)	9946(2)	8855(1)	10278(2)	45(1)
C(34)	10856(3)	8610(1)	11235(3)	58(1)
C(35)	10164(31)	8493(7)	12158(25)	99(8)
C(36)	8789(13)	8624(4)	11720(12)	69(3)
C(35′)	10113(38)	8397(9)	12045(35)	65(5)
C(36′)	9185(17)	8760(5)	12058(14)	59(3)
C(37)	8877(3)	8953(1)	10775(3)	56(1)

[a] *U*(eq) is defined as one-third of the trace of the orthogonalized U_{ij} tensor.

Table 4. Selected Bond Lengths and Angles for Pb[μ-N=C(^{t}Bu)Ph]$_3$Li·THF (**1**)

Bond Lengths (Å)			
Pb(1)–N(1)	2.33(2)	Li(1)–O(1)	1.96(3)
Pb(1)–N(2)	2.33(2)	Li(1)···Pb(1)	2.85(3)
Pb(1)–N(3)	2.33(1)	N(1)–C(11)	1.24(2)
Li(1)–N(1)	2.06(3)	N(2)–C(21)	1.32(3)
Li(1)–N(2)	2.07(2)	N(3)–C(31)	1.25(2)
Li(1)–N(3)	2.10(3)		
Bond Angles (deg)			
N(1)–Pb(1)–N(2)	81.5(5)	Li(1)–N(3)–Pb(1)	80.0(8)
N(2)–Pb(1)–N(3)	74.5(5)	Pb(1)–N(1)–C(11)	120(1)
N(3)–Pb(1)–N(1)	74.3(5)	Pb(1)–N(2)–C(21)	119(1)
N(1)–Li(1)–N(2)	95(1)	Pb(1)–N(3)–C(31)	123(1)
N(2)–Li(1)–N(3)	85(1)	Li(1)–N(1)–C(11)	154(2)
N(3)–Li(1)–N(1)	85(1)	Li(1)–N(2)–C(21)	151(2)
Li(1)–N(1)–Pb(1)	80.5(9)	Li(1)–N(3)–C(31)	156(1)
Li(1)–N(2)–Pb(1)	80.4(9)	O(1)–Li(1)···Pb(1)	169.3(1)

the core of **2** exhibits major distortions in the Sn–N and Li–N bond lengths. Thus, whereas all the Pb–N and Li–N bonds in **1** have similar values, the Sn–N bonds of **2** vary significantly in

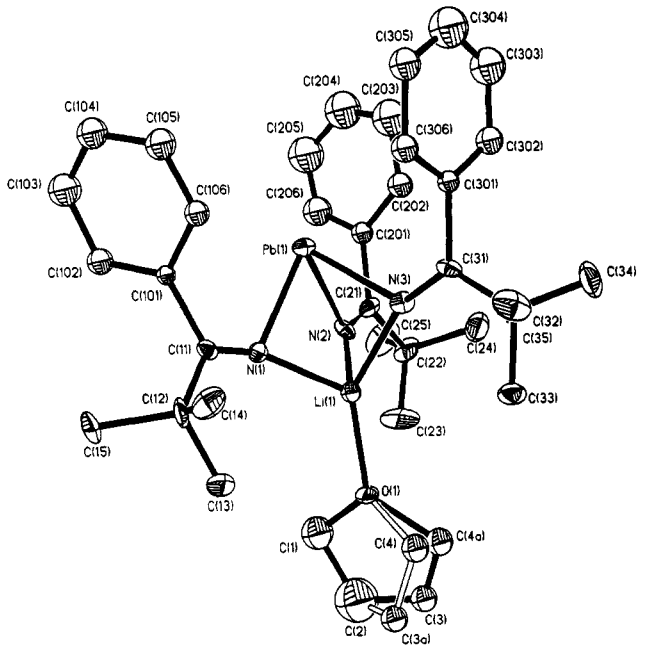

Figure 1. ORTEP plot of the monomer molecules of **1**. Thermal ellipsoids are set at the 50% level. H atoms have been omitted for clarity.

Table 5. Selected Bond Lengths and Angles for $Sn[\mu\text{-}N{=}C(^tBu)Ph]_3Li\cdot THF$ (**2**)

Bond Lengths (Å)			
Sn(1)–N(1)	2.160(2)	Li(1)–O(1)	1.964(4)
Sn(1)–N(2)	2.193(2)	Li(1)···Sn(1)	2.776(4)
Sn(1)–N(3)	2.176(2)	N(1)–C(1)	1.258(3)
Li(1)–N(1)	2.124(5)	N(2)–C(12)	1.258(3)
Li(1)–N(2)	2.048(5)	N(3)–C(23)	1.262(3)
Li(1)–N(3)	2.058(5)		
Bond Angles (deg)			
N(1)–Sn(1)–N(2)	80.38(8)	Li(1)–N(3)–Sn(1)	81.9(1)
N(2)–Sn(1)–N(3)	79.16(7)	Sn(1)–N(1)–C(1)	125.6(2)
N(3)–Sn(1)–N(1)	79.54(8)	Sn(1)–N(2)–C(12)	123.6(2)
N(1)–Li(1)–N(2)	84.6(2)	Sn(1)–N(3)–C(23)	124.6(2)
N(2)–Li(1)–N(3)	85.4(2)	Li(1)–N(1)–C(1)	153.4(2)
N(3)–Li(1)–N(1)	83.1(2)	Li(1)–N(2)–C(12)	152.9(2)
Li(1)–N(1)–Sn(1)	80.8(1)	Li(1)–N(3)–C(23)	152.8(2)
Li(1)–N(2)–Sn(1)	81.7(2)	O(1)–Li(1)···Sn(1)	169.8(2)

length [2.160(2)–2.193(2) Å] as do the Li–N bonds [2.048(5)–2.124(5) Å]. These distortions in the core bond lengths of **2** arise in order to accommodate the increased steric repulsion between the $N{=}C(^tBu)Ph$ groups surrounding the more compact core in which shorter Sn–N bonds (than the Pb–N bonds of **1**) are present.

In contrast to the tridentate linkage of the $\{Sn[\mu\text{-}N{=}C(^tBu)Ph]_3\}^-$ anion to Li^+ in **2**, a bidentate alternative is adopted by the $\{Sn(pz)_3\}^-$ anions in dimeric $[Sn(pz)_3Na\cdot 2THF(pzH)]_2$[15] in their coordination to Na^+; in so doing, these anions link two monomer units together. This is despite the fact that the N–Sn–N angle is significantly wider in the latter than in **2** (average 87°; cf. 79.7° in **2**).

An obvious difference between the structures of $Pb[\mu\text{-}N{=}C(^tBu)Ph]_3Li\cdot THF$ (**1**) and $Sn[\mu\text{-}N{=}C(^tBu)Ph]_3Li\cdot THF$ (**2**) is that there are no C—H···Sn contacts between molecules of **2** in the solid state so that the core of **2** is largely symmetrical, whereas quite extreme angular distortions occur within the core of **1** as a result of intermolecular C—H···Pb interactions. Perhaps this difference in intermolecular association is merely a reflection of the difference in atomic sizes of Sn and Pb, which allows monomers of **1** to interlock and pack more effectively than monomers of **2**, the apparent (*ortho*)C—H···Pb interactions in **1** being at best weak. However, the distortions in the core of **1** do seem very

(15) Steiner, A.; Stalke, D. *J. Chem. Soc., Chem. Commun.*, in press.

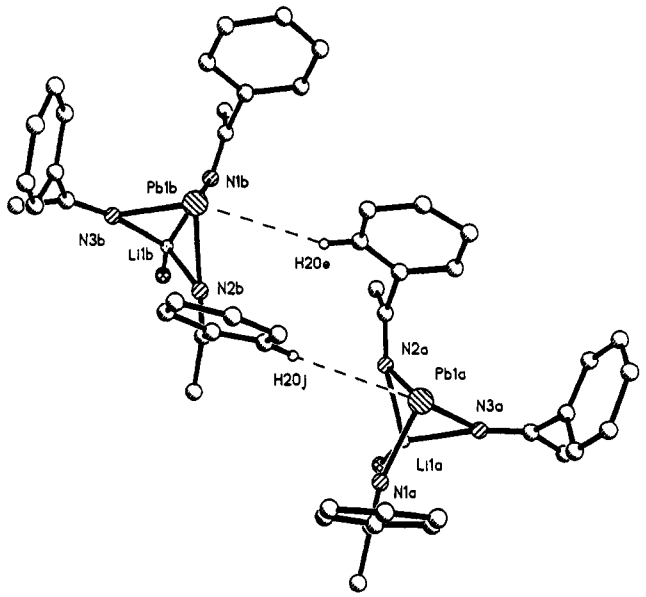

Figure 2. Association of molecules of **1** by long-range (*ortho*)C—H···Pb interactions.

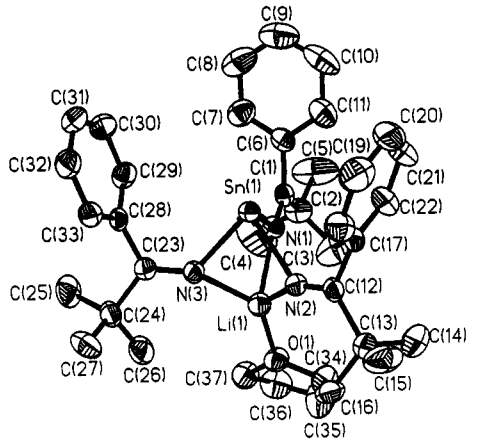

Figure 3. ORTEP plot of monomer molecules of **2**. Thermal ellipsoids are set at the 50% level. H atoms have been omitted for clarity.

large for the latter to be wholly the case. It is interesting to note, in this context, that in the crystal structure of the isoelectronic $Sb(N{=}CPh_2)_3$ complex relatively short intermolecular (*meta*)C—H···Sb contacts akin to those in **1** are present.[16] In the latter, similar angular distortions of the monomeric units, as were observed for **1**, also result in order to accommodate these interactions. At present, the magnitude and the nature (agostic or simply van der Waals) of the interactions in **1** cannot be deduced with certainty. However, the observed difference in the nature of intermolecular association between **1** and **2** may suggest that the (*ortho*)C—H···Pb contacts of **2** are more than simply van der Waals interactions.

Semiempirical (MNDO) Calculations. Semiempirical MO calculations (MNDO) were used in order to model the basic EN_3Li (E = Pb, Sn)[17] core geometries of complexes **1** and **2**. For this purpose, simple unsolvated $E(\mu\text{-}N{=}CH_2)_3Li$ (**1′** and **2′**) and solvated $E(\mu\text{-}N{=}CH_2)_3Li\cdot OMe_2$ (**1′**·OMe_2, **2′**·OMe_2) models were examined. Their enthalpies of formation (ΔH_f) and of

(16) Edwards, A. J.; Paver, M. A.; Raithby, P. R.; Russell, C. A.; Wright, D. S. *J. Chem. Soc., Dalton Trans.* **1993**, 2252.

(17) (a) C, H, N, O: Dewar, M. J. S.; Thiel, W. *J. Am. Chem. Soc.* **1977**, *99*, 4889. (b) Li (taken from MNDOC): Thiel, W. *QCPE No. 2* **1988**, *2*, 63. (c) Pb: Dewar, M. J. S.; Holloway, M. K.; Grady, G. L.; Stewart, J. J. P. *Organometallics* **1985**, *4*, 1973. (d) Dewar, M. J. S.; Holloway, M. K.; Grady, G. L.; Stewart, J. J. P. *J. Am. Chem. Soc.* **1984**, *106*, 6771.

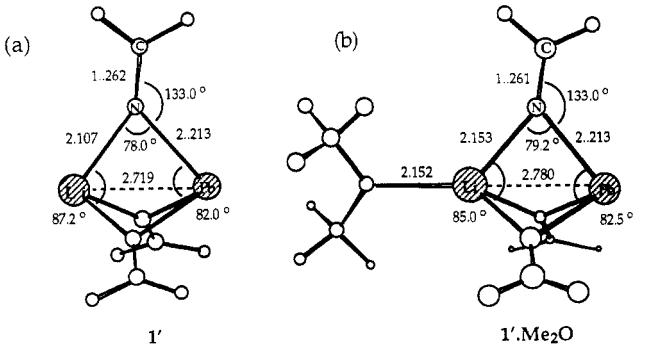

Figure 4. MNDO-optimized geometries of (a) $Pb(\mu\text{-}N{=}CH_2)_3Li$ and (b) $Pb(\mu\text{-}N{=}CH_2)_3Li{\cdot}OMe_2$.

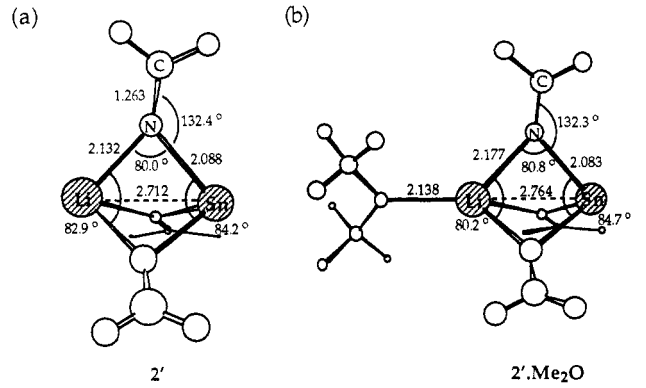

Figure 5. MNDO-optimized geometries of (a) $Sn(\mu\text{-}N{=}CH_2)_3Li$ and (b) $Sn(\mu\text{-}N{=}CH_2)_3Li{\cdot}OMe_2$.

Table 6. Enthalpies of Formation (ΔH_f) and Solvation (ΔH_s) for MNDO-Optimized Geometries of Pb and Sn Models of **1** and **2** [$\Delta H_f(Me_2O) = -50.0$ kcal mol^{-1}]

	model			
	1'	**1'**·Me_2O	**2'**	**2'**·Me_2O
ΔH_f (kcal mol^{-1})	13.7	−46.3	3.9	−57.5
ΔH_s (kcal mol^{-1})		−10.0		−11.4

solvation (ΔH_s) are shown in Table 6. The optimized geometries of the unsolvated and solvated species are shown in Figures 4 and 5.

The geometries of all the calculated models reflect well the geometries of the core structures of **1** and **2** in terms of the bond lengths and bond angles involved. Thus in the unsolvated models **1'** and **2'** the acuteness of the Li–N–Li, Li–N–E, and N–E–N angles and the close E···Li contacts match those observed in the solid-state structures of **1** and **2**, although the bond lengths in the calculated structures are typically *ca.* 0.1 Å shorter than the corresponding bond lengths in the crystal structures.[17] Solvation of **1'** and **2'** by Me_2O, giving **1'**·OMe_2 and **2'**·OMe_2, has the effect of expanding the unsolvated Pb and Sn cages. The E···Li distances in these solvated models are very similar to those seen in the structures of **1** and **2** (2.78 Å in **1'**·OMe_2, cf. *ca.* 2.85 Å in **1**; 2.76 Å in **2'**·OMe_2, cf. *ca.* 2.78 Å in **2**) as are the Li–N–E angles (78° in **1'**·OMe_2, cf. *ca.* 80° in **1**; 80.8° in **2'**·OMe_2, cf. *ca.* 82° in **2**).

Significantly, there are no bonding interactions predicted between the Pb and Sn centers and Li in any of the calculated structures. It therefore appears that the observed core geometries of **1** and **2** in the solid state largely reflect the preferred (natural) bond angles and bond lengths of the core atoms involved and that metal–metal bonding does not need to be envoked. Particularly, we believe that the preferred (very acute) Li–N–E imino bridge angle is the most major influence on the core geometries of **1** and **2**. Evidently, there is a similar degree of strain in the cores of **1'** and **2'**, judging by their similar solvation energies.

Experimental Section

All the starting materials (Cp_2Pb, Cp_2Sn, ^{t}BuLi, PhCN) and the products **1** and **2** are air and/or moisture sensitive. They were handled on a vacuum line using standard inert-atmosphere techniques[8] and under dry/O_2-free N_2. Solvents (THF, Et_2O) were dried using Na/benzophenone and degassed prior to their use in reactions. Complexes **1** and **2** were isolated and characterized with the aid of an argon-filled glovebox (Faircrest Mark 4A) fitted with an O_2 and H_2O recirculation system (Type B). Melting points were determined by using a conventional apparatus and sealing samples in capillaries under N_2. IR spectra were recorded as Nujol mulls using NaCl windows and were run on a Perkin-Elmer 2400 spectrophotometer. Elemental analyses were performed by first sealing samples in airtight aluminum boats (1–2 mg). C, H, and N analyses were carried out using a Perkin-Elmer 240 elemental analyzer. Problems were experienced in the C analysis of **1** and **2**. Despite repeated attempts, this was found to be at best ca. 1% too low for both complexes. We believe that this may be due to slight oxidation and hydrolysis of the complexes, which are extremely air and moisture sensitive, and/or to partial loss of THF of solvation, which may have occurred during the drying of the samples under vacuum before analysis. ^{1}H and ^{13}C NMR spectra were recorded on Bruker WH 250-MHz and WH 400-MHz spectrometers.

Synthesis of 1. A solution of benzonitrile (0.52 mL, 5 mmol) in 10 mL of dry THF was reacted at 0 °C with ^{t}BuLi (2.94 mL, 1.7 mol dm^{-3} in pentane, 5 mmol) under N_2. To the resulting orange solution was added Cp_2Pb (0.84 g, 2.5 mmol, in 5 mL of THF) at −30 °C. The reaction mixture was allowed to warm to room temperature and then stirred for a further 10 min. The mixture was filtered, through a porosity 4 sinter if necessary, and excess solvent was removed in vacuo until 7 mL of liquid remained, whereupon a yellow precipitate developed. This was gently warmed back into solution and stored at 5 °C for 24 h. Yellow air-sensitive crystalline rods of **1** were produced in 67% yield (relative to amount of imino ligand reacted). Mp: 62 °C. Dec: *ca.* 70 °C to black solid. Anal. Found: C, 56.5; H, 6.3; N, 5.3. Calc: C, 57.9; H, 6.5; N, 5.5. IR ν/cm^{-1} (Nujol): 3045–3076 (C—H aryl), 1616 [C=N str; cf. 1637 in (Ph)(^{t}Bu)C=NLi], 1576 (aryl C=C). Air-exposed IR spectrum/cm^{-1}: 3677 (LiO—H str), 1623 (C=N str). ^{1}H NMR (250 MHz; THF-d_8; +25 °C): *ca.* δ 7.26–6.90 (15H, groups of multiplets), 3.60 and 1.70 (8H, coordinated THF), 1.13 (27H, ^{t}Bu groups). ^{13}C NMR (100.6 MHz; THF-d_8; +25 °C): δ 175.7 (imino C), 150.0 (aryl C(1)), 128.4–126.2 (aryl C(2)–C(4)), 67.4 and 25.4 (coordinated THF), 45.3 (–*C*Me$_3$), 30.1 (–C*Me*$_3$).

Synthesis of 2. A solution of benzonitrile (0.26 mL, 2.5 mmol) in 10 mL of dry THF was reacted at 0 °C with ^{t}BuLi (1.47 mL, 1.7 mol dm^{-3} in pentane, 2.5 mmol) under N_2 to yield an orange-yellow solution. After stirring (10 min), Cp_2Sn (0.63 g, 2.5 mmol, in 1.4 mL of THF) was added, and gentle warming resulted in a yellow solution. The volume of the solvent was reduced in vacuo to 4 mL, whereupon precipitation commenced. After warming back into solution, storage (5 °C, 48 h) produced yellow crystalline blocks of **2**. Yield: 25% (after second-batch crystallization). Mp: 120 °C. Anal. Found: C, 64.3; H, 7.6; N, 6.6. Calc: C, 65.5; H, 7.4; N, 6.2. IR ν/cm^{-1} (Nujol): 3055–3040 (aryl C—H), 1636 (imino C=N). ^{1}H NMR (250 MHz; THF-d_8; +25 °C): δ 7.2–2.0 (m, Ph), 3.60 and 1.70 (coordinated THF), 1.11 (^{t}Bu). ^{13}C NMR (100.6 MHz; THF-d_8; +25 °C): δ 179.8 (imino C), 147.9 (aryl C(1)), 129.0–126.3 (aryl C(2)–C(4)), 67.4 and 25.7 (coordinated THF), 42.1 (–*C*Me$_3$), 29.1 (–C*Me*$_3$).

Synthesis of 2 from 1. Complex **2** can be prepared by the reaction between $Pb[\mu\text{-}N{=}C(^t\text{Bu})Ph]_3Li{\cdot}THF$ (0.766 g, 1 mmol) and Cp_2Sn (0.249 g, 1 mmol) in 5 mL of THF, giving a yellow solution. Addition of 5 mL of diethyl ether resulted in the precipitation of a yellow solid, which was dissolved by warming after the addition of 1 mL of THF. The solution was left for 24 h at room temperature, producing large crystalline blocks of **2** in 30% yield (first batch). The identity of the product was confirmed by infrared spectroscopy, elemental analysis, and melting point.

X-ray Structure Determinations of 1 and 2. Crystals were mounted directly from solution under Ar using a perfluorocarbon oil which protected them from atmospheric O_2 and moisture.[18] The oil "froze" at reduced temperatures and held the crystals static in the X-ray beam. Data were collected on a Siemans-Stoe AED diffractometer, and semiempirical absorption corrections based on ψ scans were employed for both complexes. Details of the structure solutions and refinements of both complexes are shown in Table 1. Both structures were solved by direct methods

(18) Kottke, T.; Stalke, D. *J. Appl. Crystallogr.* **1993**, *26*, 615.

(SHELXTl PLUS) and refined by full-matrix least-squares calculations on F^2 (SHELXL-93).[9] The Flack parameter was refined to 0.29(3)[19] for complex **2**; the high estimated standard deviation precludes any comment regarding the absolute structure. For **1**, the THF molecule exhibits disorder over C(2), C(3), and C(4), and these atoms were refined with 50% occupancy in the final cycles. Additionally, in **2** a number of light atoms showed a tendency to refine with non-positive definite anisotropic displacement parameters. These were refined in the final cycles with isotropic parameters. Atomic coordinates, bond lengths and angles, and thermal parameters for **1** and **2** have been deposited with the Cambridge Crystallographic Data Centre.

Semiempirical (MNDO) Calculations. The MNDO program used was VAMP (Dr. T. Clark, Erlangen, Germany) based on AMPAC 1.0 and MOPAC 4.0. All calculations were carried out on a CONVEX computer.[16] In all the calculational models $Li(\mu\text{-}N{=}CH_2)_3E$ and $Me_2O{\cdot}Li(\mu\text{-}N{=}CH_2)_3E$ (E = Pb, Sn), the $N{=}CH_2$ groups were refined in symmetry, giving equal bond lengths and related angles to the E and Li atoms and approximate C_{3v} core geometries.

Acknowledgment. We gratefully acknowledge the SERC (M.A.P., C.A.R., D.S.W.), the Associated Octel Co. Ltd., Ellesmere Port, U.K. (M.A.P., D.S.W.), the Royal Society (P.R.R., D.S.W.), the Nuffield Foundation (D.S.W.) and the Cambridge Crystallographic Data Centre (A.J.E.), the Fonds der Chemischen Industrie (A.S., D.S.), and the Deutsche Forschungsgemeinschaft (A.S., D.S.) for financial support. We also thank Dr. T. Clark (Erlangen, Germany) for the use of his MNDO program and Dr. R. D. Amos (Cambridge) for computing facilities.

Supplementary Material Available: Tables giving crystal data and details of the structure determinations, bond lengths, bond angles, anisotropic displacement coefficients, and hydrogen coordinates and isotropic displacement parameters for **1** and **2** (11 pages). Ordering information is given on any current masthead page.

(19) Flack, H. D. *Acta Crystallogr. Sect. A* **1983**, *37*, 876.